

Separation of the initial conditions in the inverse problem for 1D non-linear tsunami wave run-up theory*

Alexei Rybkin¹, Oleksandr Bobrovnikov¹, Noah Palmer², Daniel Abramowicz³, and Efim Pelinovsky^{4,5}

¹University of Alaska Fairbanks, Fairbanks, Alaska, United States

²University of Colorado Boulder, Boulder, Colorado, United States

³University of San Francisco, San Francisco, California, United States

⁴HSE University, Nizhny Novgorod, Russia

⁵Institute of Applied Physics, Nizhny Novgorod, Russia

April 16, 2025

Abstract

We investigate the inverse tsunami wave problem within the framework of the 1D non-linear shallow water equations (SWE). Specifically, we show that the initial displacement $\eta_0(x)$ and velocity $u_0(x)$ of the wave can be recovered, given the known motion of the shoreline $R(t)$ (the wet/dry free boundary), in terms of the Abel transform. We demonstrate that for power-shaped inclined bathymetries, this problem admits a complete solution for any η_0 and u_0 , provided the wave does not break.

It is important to note that, in contrast to the direct problem (also known as the tsunami wave run-up problem), where $R(t)$ can be computed exactly only for $u_0(x) = 0$, our algorithm can recover η_0 and u_0 exactly for any non-zero u_0 . This highlights an interesting asymmetry between the direct and inverse problems. Our results extend the work presented in [Rybkin et al., 2023, Rybkin et al., 2024], where the inverse problem was solved for $u_0(x) = 0$. As in previous work, our approach utilises the Carrier-Greenspan transformation, which linearises the SWE for inclined bathymetries. Extensive numerical experiments confirm the efficiency of our algorithms.

1 Introduction

Tsunami wave run-up is often analysed within the framework of the shallow water equations (SWE), a system of non-linear partial differential equations. In these studies, it is typically assumed that the initial water displacement and velocity of the incoming wave are known, and the objective is to compute the motion of the shoreline (also known as the dry/wet free boundary). This problem is commonly referred to as the tsunami wave run-up problem.

In this work, we are concerned with the inverse problem: determining the initial conditions (i.e., the initial displacement and velocity of the wave) based on the known motion of the shoreline. This problem has long been of practical importance for tsunami forecasting and mitigation efforts (see [Miyabe, 1934, Piatanesi et al., 2001, Pires and Miranda, 2003, Voronin et al., 2015, Satake, 2022] and the literature cited therein). Since tsunami waves are governed by non-linear PDEs, the inverse tsunami wave problem poses a significant challenge. Thus, it is critical to develop reasonable models where this problem can be solved effectively.

In [Rybkin et al., 2023], it was demonstrated that for a sloping plane beach, the initial displacement of the wave can be recovered under the assumption of zero initial velocity. More recently, in [Rybkin et al., 2024], this result was extended to bays with inclined power-shaped cross-sections. Such three-dimensional bathymetries can be parametrised by a single function of one variable (see [Rybkin et al., 2021], for precise definitions and statements). However, the assumption of zero initial velocity has remained unaddressed, limiting applicability to real-life scenarios where initial velocity plays a major role (e.g., tsunamis caused by underwater

*To appear in Studies in Applied Mathematics

landslides). In such cases, the initial displacement is often negligible instead. In [Rybkin et al., 2024], this case was left as an open problem.

In this paper, we provide a complete solution to the inverse problem for inclined power-shaped bays where both the initial displacement and initial velocity are non-zero. While our approach follows the framework established in [Rybkin et al., 2024], two new insights are critical to our results, which we summarise below at a non-technical level.

The first insight concerns a key difference between the direct and inverse problems. For context, as in [Rybkin et al., 2024], we use the Carrier-Greenspan hodograph transformation to linearise the shallow water equations into a specific form of the linear wave equation. This allows us to apply standard techniques from mathematical physics. Relevant works in this context include those by [Shimozono, 2016], [Pedersen, 2021], [Synolakis and Bernard, 2006], and [Aydin, 2020] on SWE in power-shaped bays and plane beaches. For numerical treatment of channels of arbitrary cross-sections, we refer the reader to works of [Hernández-Dueñas and Karni, 2011], [Hadiarti et al., 2023], [Welahettige et al., 2018], and [Wang et al., 2019]. For a different kind of inverse problems for shallow water equations we suggest the recent work of [Hakl and Torres, 2025].

However, while the Carrier-Greenspan linearisation simplifies the problem, it introduces a challenge: the initial conditions in the hodograph plane are specified on a curve that depends on the initial conditions themselves. This curve becomes a straight line only if the initial velocity is zero, which is a well-documented issue in hodograph transformations (e.g., [Johnson, 1997]). In prior studies, this issue was addressed under additional assumptions (see [Carrier et al., 2003]; [Kânoğlu and Synolakis, 2006]). In [Nicolisky et al., 2018], we introduced the data projection method, which offers a robust solution for non-zero initial velocity. This method, further developed in [Rybkin et al., 2021], approximates initial conditions in the hodograph plane using Taylor’s formula along a straight line, ensuring the solutions to the original and modified problems are as close as desired (though not exact).

For the inverse problem considered here, such complications are absent. The initial conditions can be recovered exactly as long as the Carrier-Greenspan transformation remains invertible. This leads to a surprising asymmetry between the direct and inverse problems, which appears to be a new phenomenon.

Our second novel insight is both surprising and counter-intuitive. A detailed analysis of our formulas reveals that, in the hodograph plane, the new dependent variables (interpreted physically as pressure and velocity) uniquely contribute to the solution at the shoreline, a fixed point in the hodograph plane. This allows the recovery of both the initial displacement and the initial velocity from the shoreline motion, which is described by a single function, referred to as the shoreline data or run-up function. It is particularly striking that two independent initial conditions can be deduced from a single function – a phenomenon we term the “separation of initial conditions at the shoreline”. The run-up function separates contributions from the initial displacement and initial velocity. In practical applications, when the run-up is derived from measurements, this separation can only be approximate.

The remainder of this work is organised as follows: in Section 2 the mathematical model is introduced; in Section 3 we derive the solution to the direct problem. We present and discuss the phenomenon of the separation of the initial conditions at the shoreline in Section 4. Section 5 provides a complete solution to the inverse problem for inclined power-shaped bays when both initial displacement and initial velocity are non-zero. Some remarks left outside of the main body are given in Section 6. Finally, we provide a numerical experiment which validates our findings and concluding remarks in Sections 7 and 8 respectively.

2 Mathematical model

The 1D shallow water (Saint-Venant) equations, given in dimensionless units as

$$\begin{aligned} \partial_t \eta + u \partial_x (x + \eta) + \frac{m}{m+1} (x + \eta) \partial_x u &= 0, & (\text{mass}) \\ \partial_t u + u \partial_x u + \partial_x \eta &= 0, & (\text{momentum}) \end{aligned} \tag{1}$$

govern water motion in an infinite parabolic-shaped bathymetry (see Figure 1) under the assumptions of no vorticity, no friction, no dispersion, and no wave breaking. Here $u(x, t)$ is the depth averaged flow velocity over the corresponding cross-section, $\eta(x, t)$ is the water displacement exceeding the unperturbed water

level, and m is the bay parameter. The substitution

$$\tilde{x} = \frac{H_0}{\alpha} x, \quad \tilde{t} = \sqrt{\frac{H_0}{g}} \frac{t}{\alpha}, \quad \tilde{\eta} = H_0 \eta, \quad \tilde{u} = \sqrt{H_0 g} u, \quad (2)$$

where H_0 is the characteristic height of the wave, α is the slope of the bathymetry, and g is the acceleration of gravity, turns the dimensionless system into one with dimension (dimensional variables are the ones with tildes). There are two fundamental difficulties associated with the system (1): non-linearity and the free boundary. As a result of water motion, the shoreline is shifting; let us denote the law of *vertical* motion of the shoreline as $R(t)$. Typically the system (1) is considered together with the initial conditions

$$u(x, 0) = u_0(x), \quad \eta(x, 0) = \eta_0(x) \quad (3)$$

and the goal is to compute the vertical run-up of the wave $R(t)$. We call this the direct or forward problem.

3 Solution to the forward problem

In this section we outline a solution to the forward problem. The forward problem is well-studied both numerically [Hartle et al., 2021, Bueler-Faudree et al., 2022] and analytically [Pelinovsky and Mazova, 1992, K  noğlu and Synolakis, 2006, Rybkin et al., 2014, Didenkulova and Pelinovsky, 2011a, Carrier and Greenspan, 1958]. Our solution to the forward problem here mostly follows the solution of [Rybkin et al., 2021].

The Carrier-Greenspan hodograph transformation (CGT), originally introduced for the sloping plane beach by [Carrier and Greenspan, 1958] and later generalised for power-shaped bays by [Rybkin et al., 2014], allows one to linearise (1) and fix the free boundary. Specifically, this transform introduces new variables σ, τ and new functions ψ, φ as

$$\begin{aligned} \sigma = x + \eta(x, t), \quad \tau = t - u(x, t), \quad \varphi(\sigma, \tau) = u(x, t), \quad \psi(\sigma, \tau) = \eta(x, t) + u^2(x, t)/2. \\ \text{(total height)} \quad \quad \text{(delayed time)} \quad \quad \text{(velocity)} \quad \quad \text{(pressure)} \end{aligned} \quad (4)$$

Physically, σ is interpreted as the total height of the wave, τ as the delayed time, φ as the velocity and ψ as the pressure (from Bernoulli's equation).

Like most of hodograph transformations, the CGT complicates the initial conditions. Indeed, when we set $t = 0$ in the equation $\tau = t - u(x, t)$, we see that τ is not (identically) zero unless $u(x, 0) = 0$. In the hodograph plane (σ, τ) the initial conditions are specified on a parametric curve which we denote $\tau = \gamma(\sigma)$. The system (1) together with (3) under (4) becomes

$$\begin{aligned} \partial_\tau \psi + \frac{m}{m+1} \sigma \partial_\sigma \varphi + \varphi &= 0, \\ \partial_\tau \varphi + \partial_\sigma \psi &= 0, \\ \psi(\sigma, \gamma(\sigma)) &= \eta_0 + u_0^2/2 =: \psi_{\text{phys}}(\sigma), \\ \varphi(\sigma, \gamma(\sigma)) &= u_0 =: \varphi_{\text{phys}}(\sigma). \end{aligned} \quad (5)$$

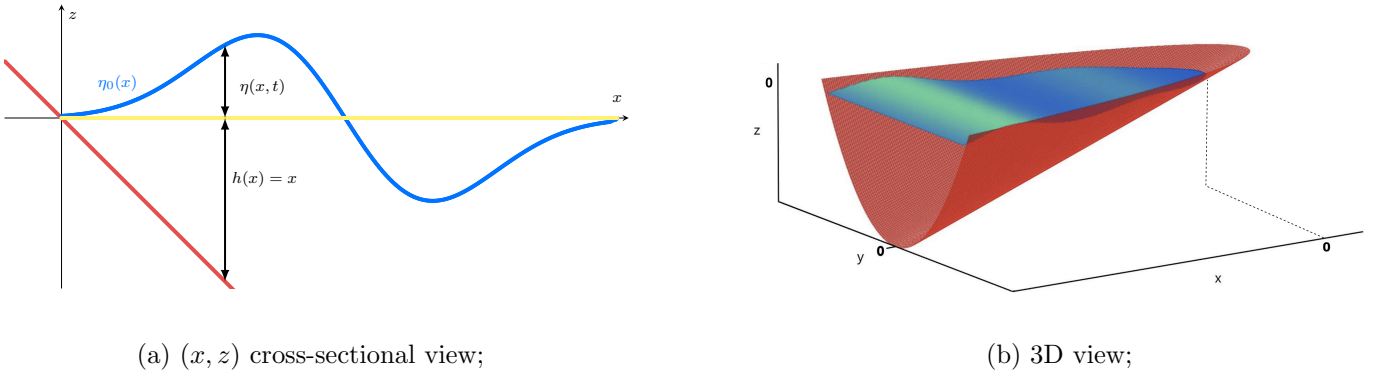


Figure 1: A sketch of the parabolic bay geometry. The bathymetry $z(x, y) = -x + |y|^m$ is in red, the unperturbed water level is in yellow, an the water level is in blue. The total perturbed water depth is given by $H(x, t) = h(x) + \eta(x, t)$.

Note that this is a linear hyperbolic system. The method of data projections [Rybkin et al., 2021] allows one to replace the initial conditions on γ with initial conditions on the line $\tau = 0$ such that the solution to the original and the solution to the new IVP are arbitrarily close. To give the reader an understanding of the complexity of the method we give the formula for the n -th order projection:

$$\begin{pmatrix} \varphi_n(\sigma) \\ \psi_n(\sigma) \end{pmatrix} = \begin{pmatrix} \varphi_{\text{phys}}(\sigma) \\ \psi_{\text{phys}}(\sigma) \end{pmatrix} + \sum_{k=1}^n \frac{\varphi_{\text{phys}}^k(\sigma)}{k!} [D\Delta]^k \begin{pmatrix} \varphi_{\text{phys}}(\sigma) \\ \psi_{\text{phys}}(\sigma) \end{pmatrix}, \quad (6)$$

where

$$D = \begin{pmatrix} 1 & \varphi'_{\text{phys}}(\sigma) \\ \frac{m\sigma}{m+1} & 1 \end{pmatrix} \varphi'_{\text{phys}}(\sigma), \quad \Delta = - \begin{pmatrix} 0 & 1 \\ \frac{m\sigma}{m+1} & 0 \end{pmatrix} \partial_\sigma - \begin{pmatrix} 0 & 0 \\ 1 & 0 \end{pmatrix}. \quad (7)$$

Using (6) the IVP (5) becomes

$$\begin{aligned} \partial_\tau \psi + \frac{m}{m+1} \sigma \partial_\sigma \varphi + \varphi &= 0, \\ \partial_\tau \varphi + \partial_\sigma \psi &= 0, \\ \psi(\sigma, 0) &= \psi_{\text{proj}}(\sigma), \\ \varphi(\sigma, 0) &= \varphi_{\text{proj}}(\sigma). \end{aligned} \quad (8)$$

Here $\varphi_{\text{proj}}, \psi_{\text{proj}}$ are found from u_0, η_0 using the infinite order data projection so that the solutions to (5) and (8) are *exactly* the same. Note that it is impossible to find these initial conditions from the physical initial conditions exactly when solving the forward problem since Taylor's series is truncated when doing data projections. The linear hyperbolic system (8) then can be written as a wave equation

$$\partial_\tau^2 \psi = \frac{m}{m+1} \sigma \partial_\sigma^2 \psi + \partial_\sigma \psi, \quad (9)$$

which can be solved using the Fourier-Bessel transform. Returning back to the hyperbolic system (8) one obtains the solution

$$\begin{aligned} \psi(\sigma, \tau) = 2\sigma^{-\frac{1}{2m}} \int_0^\infty k \left\{ \int_0^\infty \psi_{\text{proj}}(s) s^{\frac{1}{2m}} J_{\frac{1}{m}}(2k\sqrt{s}) ds \cos(\omega k\tau) \right. \\ \left. - \omega \int_0^\infty \varphi_{\text{proj}}(s) s^{\frac{1}{2m}+\frac{1}{2}} J_{\frac{1}{m}+1}(2k\sqrt{s}) ds \sin(\omega k\tau) \right\} J_{\frac{1}{m}}(2k\sqrt{\sigma}) dk, \end{aligned} \quad (10)$$

$$\begin{aligned} \varphi(\sigma, \tau) = \frac{2}{\omega} \sigma^{-\frac{1}{2m}-\frac{1}{2}} \int_0^\infty k \left\{ \int_0^\infty \psi_{\text{proj}}(s) s^{\frac{1}{2m}} J_{\frac{1}{m}}(2k\sqrt{s}) ds \sin(\omega k\tau) \right. \\ \left. + \omega \int_0^\infty \varphi_{\text{proj}}(s) s^{\frac{1}{2m}+\frac{1}{2}} J_{\frac{1}{m}+1}(2k\sqrt{s}) ds \cos(\omega k\tau) \right\} J_{\frac{1}{m}+1}(2k\sqrt{\sigma}) dk, \end{aligned} \quad (11)$$

where $\omega = \sqrt{m/(m+1)}$ and J_ν is the Bessel function of the first kind of order ν . Taking $\sigma \rightarrow 0$ in (10) one obtains the relation that we call the shoreline equation

$$\begin{aligned} \psi(0, \tau) = \frac{4}{\Gamma(1+\frac{1}{m})} \int_0^\infty k^{1+\frac{1}{m}} \left\{ \int_0^\infty \hat{\psi}_{\text{proj}}(\lambda) \lambda^{\frac{1}{m}+1} J_{\frac{1}{m}}(2k\lambda) d\lambda \cos(\omega k\tau) \right. \\ \left. - \omega \int_0^\infty \hat{\varphi}_{\text{proj}}(\lambda) \lambda^{\frac{1}{m}+2} J_{\frac{1}{m}+1}(2k\lambda) d\lambda \sin(\omega k\tau) \right\} dk, \end{aligned} \quad (12)$$

where $\lambda = \sqrt{s}$, $\hat{\psi}_{\text{proj}}(\lambda) = \psi_{\text{proj}}(\lambda^2)$ and $\hat{\varphi}_{\text{proj}}(\lambda) = \varphi_{\text{proj}}(\lambda^2)$. The run-up $R(t)$ can be found from $\psi(0, \tau)$ using (4), which at the shore reads as

$$\tau = t + \partial_t R(t), \quad \varphi(0, \tau) = -\partial_t R(t), \quad \psi(0, \tau) = R(t) + \frac{1}{2}(\partial_t R(t))^2. \quad (13)$$

Note that here we take advantage of dealing with dimensionless units: at the free boundary we have $\eta(x, t) = R(t)$ and $u(x, t) = -\partial_t R(t)$ since the slope of the bathymetry is $\pi/4$. This concludes the solution to the forward problem.

4 Separation of the initial conditions at the shoreline

In this section we present two propositions which describe the relationship between the pressure and velocity at the shoreline and allow for the separation of the initial conditions at the shoreline. First, like in the derivation of (12), taking $\sigma \rightarrow 0$ in (11) yields

$$\begin{aligned} \varphi(0, \tau) = \frac{4}{\omega \Gamma(2 + \frac{1}{m})} \int_0^\infty k^{2 + \frac{1}{m}} & \left\{ \int_0^\infty \widehat{\psi}_{\text{proj}}(\lambda) \lambda^{1 + \frac{1}{m}} J_{\frac{1}{m}}(2k\lambda) d\lambda \sin(\omega k\tau) \right. \\ & \left. + \omega \int_0^\infty \widehat{\varphi}_{\text{proj}}(\lambda) \lambda^{\frac{1}{m} + 2} J_{\frac{1}{m} + 1}(2k\lambda) d\lambda \cos(\omega k\tau) \right\} dk. \end{aligned} \quad (14)$$

Comparing (12) and (14) we observe that the velocity φ at the shoreline can be re-expressed as the derivative of ψ . This leads us to the following important observation.

Proposition 1. *The pressure ψ and velocity φ from (4) are related at the shoreline ($\sigma = 0$) by*

$$\varphi(0, \tau) = -\partial_\tau \psi(0, \tau). \quad (15)$$

Next, we examine (12). Note that under the outer integral there is a sum of even and odd functions with respect to τ . This suggests that if $\psi(0, \tau)$ could be split into its even and odd components, it would be possible to uncouple $\widehat{\psi}_{\text{proj}}$ and $\widehat{\varphi}_{\text{proj}}$:

$$\begin{aligned} [\psi(0, \tau)]_{\text{even}} &= \frac{4}{\Gamma(1 + \frac{1}{m})} \int_0^\infty k^{1 + \frac{1}{m}} \int_0^\infty \widehat{\psi}_{\text{proj}}(\lambda) \lambda^{\frac{1}{m} + 1} J_{\frac{1}{m}}(2k\lambda) d\lambda \cos(\omega k\tau) dk, \\ [\psi(0, \tau)]_{\text{odd}} &= \frac{-4\omega}{\Gamma(1 + \frac{1}{m})} \int_0^\infty k^{1 + \frac{1}{m}} \int_0^\infty \widehat{\varphi}_{\text{proj}}(\lambda) \lambda^{\frac{1}{m} + 2} J_{\frac{1}{m} + 1}(2k\lambda) d\lambda \sin(\omega k\tau) dk. \end{aligned} \quad (16)$$

Here we mean even/odd in the usual sense: the function f is even if $f(x) = f(-x)$ and is odd if $f(x) = -f(-x)$. To allow such separation we assume $R(t)$ to be a real analytic function (that is, to have a convergent Taylor series in the entire complex plane). The physical domain of $R(t)$ is narrower. Analyticity of $R(t)$ together with (13) easily implies analyticity of $\psi(0, \tau)$ and $\varphi(0, \tau)$, as long as the CGT is invertible. We arrive at our second statement.

Proposition 2. *Let $R(t)$ be an analytic function that fits the shoreline run-up data. Assume that the CGT is invertible, and so the wave does not break. Then the even component of the pressure at the shoreline $\psi(0, \tau) = R(t) + (\partial_t R(t))^2/2$, where $t = \tau + \varphi(0, \tau) = \tau - \partial_t R(t)$, depends only on the initial pressure of the wave and the odd component depends only on the initial velocity of the wave.*

It is worth mentioning that analyticity is a sufficient condition, but not necessary. To allow separation we only need a reasonable way to split a function into its even and odd components.

5 Inverse problem

We now consider the full inverse problem. Given the shoreline oscillations $R(t)$, we recover the initial velocity u_0 and displacement η_0 . Since the conversion of $R(t)$ to $\psi(0, \tau)$ is trivial, there are two steps in the solution to our inverse problem:

- (1) from $\psi(0, \tau)$ recover $\psi_{\text{proj}}, \varphi_{\text{proj}}$;
- (2) from ψ_{proj} and φ_{proj} find η_0 and u_0 .

The equations in (16) can be inverted using inverse Fourier transforms together with the integral representation of the Bessel function. However, for $\widehat{\varphi}_{\text{proj}}$ it is more convenient to separate $\varphi(0, \tau)$ in a similar

manner to that done for $\psi(0, \tau)$ to obtain an expression for $\widehat{\varphi}_{\text{proj}}$ in terms of an integral of the even component of $\varphi(0, \tau)$. From this one obtains

$$\widehat{\psi}_{\text{proj}}(\lambda) = \frac{2\sqrt{\pi}\Gamma(1+1/m)}{\lambda\Gamma(1/m+1/2)} \int_0^{\lambda/\pi} \left(1 - \left(\frac{\pi\xi}{\lambda}\right)^2\right)^{1/m-1/2} \Psi(\xi) d\xi, \quad (17)$$

$$\widehat{\varphi}_{\text{proj}}(\lambda) = \frac{2\sqrt{\pi}\Gamma(2+1/m)}{\lambda^{2+2/m}\Gamma(3/2+1/m)} \int_0^{\lambda/\pi} (\lambda^2 - \pi^2\xi^2)^{1/m+1/2} \Phi(\xi) d\xi, \quad (18)$$

where $\Psi(\xi) := \psi_{\text{even}}(0, q\xi)$, $\Phi(\xi) := \varphi_{\text{even}}(0, q\xi)$, $q = 2\pi/\omega$, and $\xi = \tau/q$. This completes the first step in the solution of the inverse problem: from the energy at the shoreline $\psi(0, \tau)$ we recover the initial conditions ψ_{proj} and φ_{proj} in the hodograph (σ, τ) plane using (17) and (18) respectively. This recovery is exact in the following sense: precisely these initial conditions on $\tau = 0$ in the hodograph plane produce the observed $R(t)$. In contrast, when solving the direct problem it is impossible to obtain these conditions (on $\tau = 0$) from $\eta_0(x)$ and $u_0(x)$ exactly since the method of data projections truncates the Taylor series.

Exact recovery of the initial conditions in the physical plane

Now we recover the initial conditions u_0 and η_0 in physical space. From (10, 11) we find $\psi(\sigma, \tau)$ and $\varphi(\sigma, \tau)$ (their values for *all* values (σ, τ)) and then perform the inverse CGT. We first need to find the curve γ . Note that on γ (equivalently at $t = 0$) we have from (4) that $\gamma(\sigma) = \tau = -u(x, 0) = -\varphi(\sigma, \gamma(\sigma))$. Hence, the curve $\gamma(\sigma)$ can be found by solving $\gamma(\sigma) = -\varphi(\sigma, \gamma(\sigma))$ for γ . It is left to find the initial conditions in the physical space from (4) as

$$\begin{aligned} \eta_0(x) &= \psi(\sigma, \gamma(\sigma)) - \varphi^2(\sigma, \gamma(\sigma))/2, & u_0(x) &= \varphi(\sigma, \gamma(\sigma)), \\ x &= \sigma - \psi(\sigma, \gamma(\sigma)) + \varphi^2(\sigma, \gamma(\sigma))/2. \end{aligned} \quad (19)$$

The uniqueness of this process follows from the invertibility of the CGT.

In conclusion, the the inverse problem can be solved exactly without using the method of data projection, which as can be seen in (6) is quite involved. Moreover, we are able to recover both the initial displacement η_0 and initial velocity u_0 from just the shoreline oscillations $R(t)$, which is counter-intuitive at first sight.

6 Remarks

In this section we point out several important assumptions and details. In our derivations we assume the CGT to be invertible. Mathematically it means that the Jacobians

$$\det \frac{\partial(\sigma, \tau)}{\partial(x, t)}, \quad \det \frac{\partial(x, t)}{\partial(\sigma, \tau)} \quad (20)$$

do not vanish. Physically it means that the wave does not break [Rybkin et al., 2014].

We assume $R(t)$ to be an analytic function. In practice, the shoreline data would be given as a set of measurements. In that case analytic approximation must be employed first. For example, a wave-like data can be approximated as a finite sum of Gaussian pulses:

$$\overline{R}(t) = \sum a_j e^{-b_j(t-c_j)^2}, \quad (21)$$

where $a_j, c_j \in \mathbb{R}$ and $b_j > 0$.

When we recover the curve $\gamma(\sigma)$ in the hodograph plane we first recover ψ, φ in the entire (σ, τ) plane. While this makes perfect sense mathematically, it is impossible to do numerically. Instead one should estimate how far $\gamma(\sigma)$ is from $\tau = 0$ based on the computed φ_{proj} , next compute ψ, φ on a grid (σ_j, τ_i) , and then for each σ_j find τ_{i_j} that minimises $f(\tau) = |\tau + \varphi(\sigma_j, \tau)|$. Then set $\gamma(\sigma_j) := \tau_{i_j}$. Higher accuracy can be achieved by refining the grid around the curve found and repeating this process.

Finally, we note that the integral transforms derived in (17) and (18) are a special form of the Abel transform, which finds its applications in various fields, such as image processing, tomography, and astronomy, especially in context of inverse problems [Epstein, 2007, Deans, 2007, de Hoop and Ilmavirta, 2017]. In our derivations it appears as the composition of the Fourier and Hankel transform; this result is known as the projection-slice theorem [Bracewell, 2003].

7 Verification

For numerical verification we manufacture the solution to the inverse problem. We take $R(t)$ generated via the forward solution from three different initial conditions, a Gaussian pulse, a soliton wave, and an N-wave,

$$\begin{aligned}\eta_0(x) &= 0.00005e^{-3(x-3)^2}, \\ \eta_0(x) &= 0.00005 \operatorname{sech}^2(2x - 6), \\ \eta_0(x) &= 0.00005e^{-3(x-3)^2} - 0.000025e^{-2(x-4)^2},\end{aligned}\tag{22}$$

and in all three cases we assume the velocity to be

$$u_0(x) = -2\sqrt{\frac{m+1}{m}} \left(\sqrt{\eta_0(x) + x} - \sqrt{x} \right).\tag{23}$$

For such a velocity it was shown by [Didenkulova and Pelinovsky, 2011b] that the wave propagates towards the shore. Starting with (22) and (23) the shoreline oscillations can be computed using the solution to the forward problem. This solution to the forward problem was numerically verified against the so-called augmented shallow water equations system by [Valiani and Caleffi, 2024]. After the run-up is found from the solution to the forward problem, we find $\psi(0, \tau)$ and $\varphi(0, \tau)$ from (13). The initial conditions in the hodograph plane can then be computed from (17) and (18). After that we solve the forward problem by (10) and (11). Finally, following the method described in Section 6 we recover the curve $\gamma(\sigma)$ and the initial conditions on it. Figures 2, 3, and 4 demonstrate the original and the recovered initial conditions. We see that our model captures the key features of the wave. We observe that our algorithm performs better on the N-wave, than on the Gaussian or soliton wave. We believe, this happens due to the numerical error build-up, which is more noticeable in cases of sign-constant waves (Gaussian and soliton).

While our results here are mainly analytical, we briefly discuss the computational cost of the proposed algorithm.

Given the run-up data $R(t)$ as an N -dimensional vector of measurements, we find $\psi(0, \tau)$ and $\varphi(0, \tau)$ from (13) using numerical differentiation and pointwise algebraic operations with arrays (vectors). For our next step we implement numerical integration for equations (17) and (18) in order to find $\psi(\sigma, 0)$ and $\varphi(\sigma, 0)$. While the current quadrature is $O(N^2)$, these integral transforms are compositions of the Fourier and Hankel transforms, so the integration can be implemented using the FFT and FHT at the cost $O(N \log N)$. Then, in order to perform the inverse CGT we need to compute ψ and φ from (10) and (11). This again can be done using the FFT and FHT for all σ, τ , so the computational cost would be $O(N^2 \log N)$, but the current slow implementation is $O(N^4)$. Next, we recover the curve γ . Using brute force to solve the minimisation problem for γ described in Section 6 is $O(N^2)$. Finally, once γ is found, the inverse CGT is performed using pointwise algebraic operations with vectors. Thus, if FFT and FHT algorithms are applied then the total cost is $O(N^2 \log N)$.

8 Conclusions

We have shown that for the 1D non-linear shallow water equations in power-shaped bays, there exists a relationship between the hodograph functions at the shore, which allows for the recovery of both the initial displacement and velocity from the shoreline oscillations. Moreover, in the hodograph plane the initial displacement and velocity give distinguishable contributions to the run-up. This result is surprising, as it is unexpected that both the initial conditions can be recovered from a single function $R(t)$. Numerical experiments demonstrate good agreement between the original and the recovered initial condition. Finally, we have shown that the inverse problem can be solved exactly, without loss of accuracy due to the projections, unlike the direct problem.

Acknowledgements

Alexei Rybkin, Oleksandr Bobrovnikov, Noah Palmer, and Daniel Abramowicz acknowledge support from NSF grant DMS-2307774. Efim Pelinovsky's research is supported by the RSF grant 24-47-02007 (section 3).

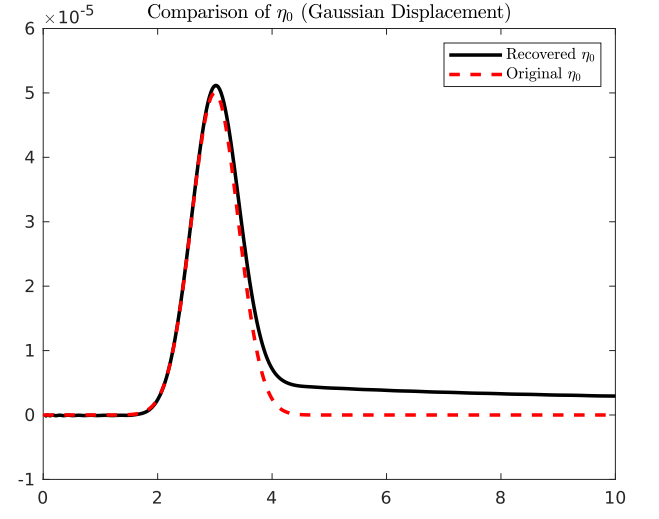
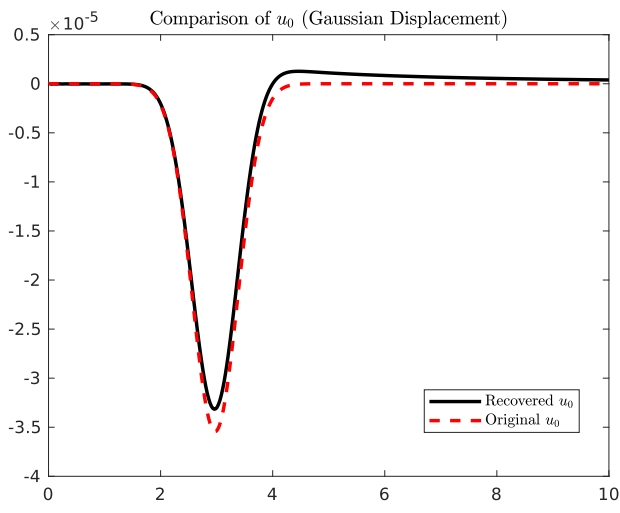


Figure 2: Comparison of the original initial conditions to the recovered initial conditions for a Gaussian wave.

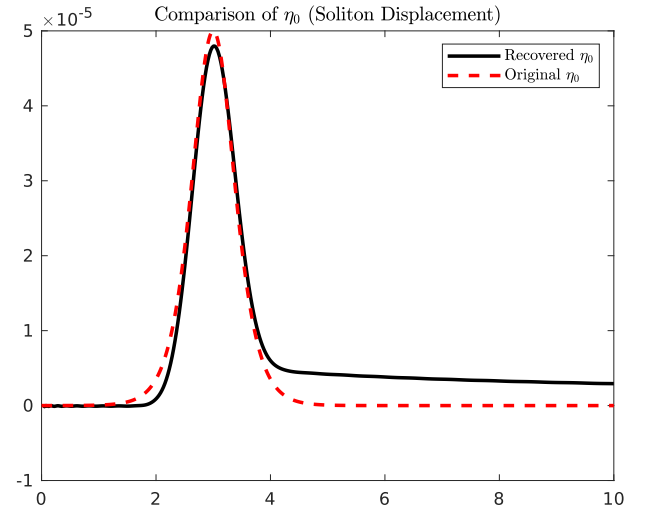
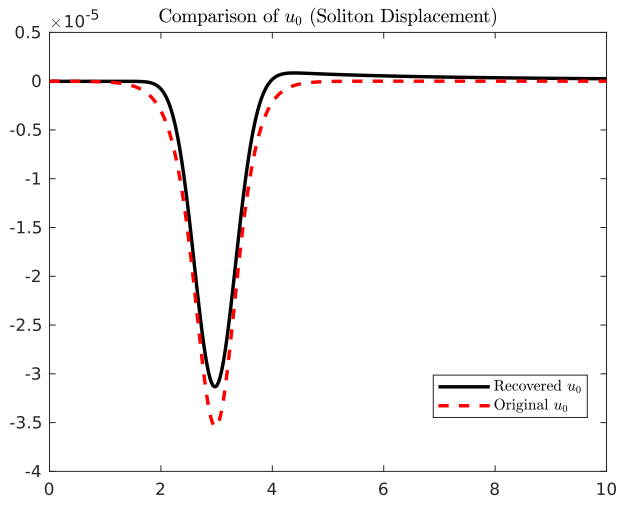


Figure 3: Comparison of the original initial conditions to the recovered initial conditions for a soliton wave.

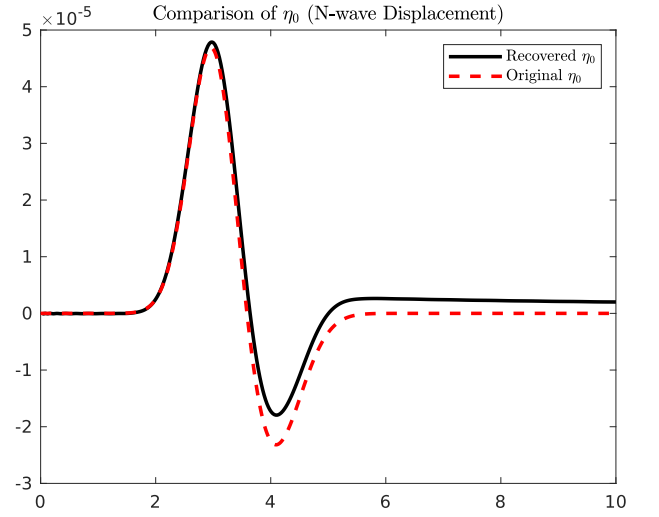
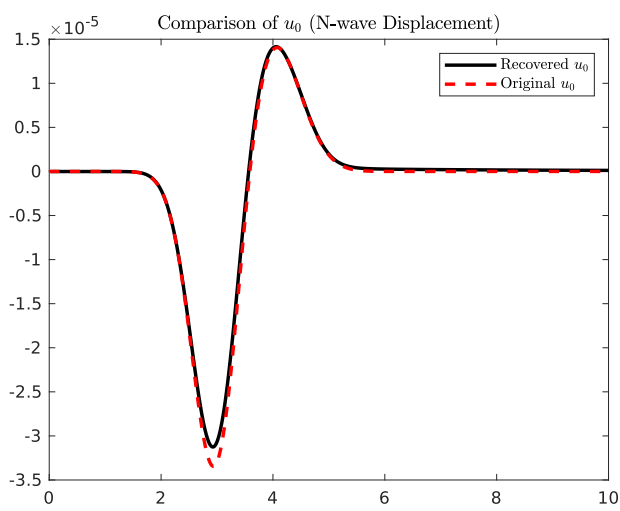


Figure 4: Comparison of the original initial conditions to the recovered initial conditions for an N-wave.

Data availability

No data was used for the research described in the article.

References

- [Aydin, 2020] Aydin, B. (2020). On open boundary conditions for long wave equation in the hodograph plane. *Physics Letters A*, 384(13):126258.
- [Bracewell, 2003] Bracewell, R. (2003). *The Projection-Slice Theorem*, pages 493–504. Springer US, Boston, MA.
- [Bueler-Faudree et al., 2022] Bueler-Faudree, T., Delamere, S., Dutykh, D., Rybkin, A., and Suleimani, A. (2022). Fast shallow water-wave solver for plane inclined beaches. *SoftwareX*, 17.
- [Carrier and Greenspan, 1958] Carrier, G. and Greenspan, H. (1958). Water waves of finite amplitude on a sloping beach. *J. Fluid Mech.*, 1:97–109.
- [Carrier et al., 2003] Carrier, G., Wu, T., and Yeh, H. (2003). Tsunami run-up and draw-down on a plane beach. *J. Fluid Mech.*, 475:79–99.
- [de Hoop and Ilmavirta, 2017] de Hoop, M. V. and Ilmavirta, J. (2017). Abel transforms with low regularity with applications to x-ray tomography on spherically symmetric manifolds. *Inverse Problems*, 33(12):124003.
- [Deans, 2007] Deans, S. (2007). *The Radon Transform and Some of Its Applications*. Dover Books on Mathematics Series. Dover Publications.
- [Didenkulova and Pelinovsky, 2011a] Didenkulova, I. and Pelinovsky, E. (2011a). Non-linear wave evolution and runup in an inclined channel of a parabolic cross-section. *Phys. Fluids*, 23(8).
- [Didenkulova and Pelinovsky, 2011b] Didenkulova, I. and Pelinovsky, E. (2011b). Rogue waves in nonlinear hyperbolic systems (shallow-water framework). *Nonlinearity*, 24(3).
- [Epstein, 2007] Epstein, C. L. (2007). *Introduction to the Mathematics of Medical Imaging*. Society for Industrial and Applied Mathematics, Philadelphia, PA, 2 edition.
- [Hadiarti et al., 2023] Hadiarti, R. N., Pudjaprasetya, S. R., and Swastika, P. V. (2023). The momentum-conserving simulation for shallow water flows in channels with arbitrary cross-sections. *European Journal of Mechanics - B/Fluids*, 99:74–83.
- [Hakl and Torres, 2025] Hakl, R. and Torres, P. J. (2025). The inverse problem for periodic travelling waves of the linear 1d shallow-water equations. *Physica D: Nonlinear Phenomena*, 472:134496.
- [Hartle et al., 2021] Hartle, H., Rybkin, A., Pelinovsky, E., and Nicolsky, D. (2021). Robust computations of runup in inclined U- and V-shaped bays. *Pure Appl. Geophys.*, 178:5017–5029.
- [Hernández-Dueñas and Karni, 2011] Hernández-Dueñas, G. and Karni, S. (2011). Shallow water flows in channels. *Journal of Scientific Computing*, 48(1):190–208.
- [Johnson, 1997] Johnson, R. (1997). *A modern introduction to the mathematical theory of water waves*. Cambridge University Press.
- [Kânoğlu and Synolakis, 2006] Kânoğlu, U. and Synolakis, C. (2006). Initial value problem solution of non-linear shallow water-wave equations. *Phys. Rev. Lett.*, 97.
- [Miyabe, 1934] Miyabe, N. (1934). An investigation of the Sanriku tsunami based on mareogram data. *Bull. Earthq. Res. Inst., Univ. Tokyo*, 1:112–126.
- [Nicolsky et al., 2018] Nicolsky, D., Pelinovsky, E., Raz, A., and Rybkin, A. (2018). General initial value problem for the non-linear shallow water equations: Runup of long waves on sloping beaches and bays. *Phys. Lett. A*, 318(38):2738–2743.
- [Pedersen, 2021] Pedersen, G. K. (2021). Asymptotic, convergent, and exact truncating series solutions of the linear shallow water equations for channels with power law geometry. *SIAM Journal on Applied Mathematics*, 81(2):285–303.

- [Pelinovsky and Mazova, 1992] Pelinovsky, E. and Mazova, R. (1992). Exact analytical solutions of nonlinear problems of tsunami wave run-up on slopes with different profiles. *Natural Hazards*, 6(3):227–249.
- [Piatanesi et al., 2001] Piatanesi, A., Tinti, S., and Pagnoni, G. (2001). Tsunami waveform inversion by numerical finite-elements Green’s functions. *Natural Hazards and Earth System Sciences*, 1(4):187–194.
- [Pires and Miranda, 2003] Pires, C. and Miranda, P. M. A. (2003). Sensitivity of the adjoint method in the inversion of tsunami source parameters. *Natural Hazards and Earth System Sciences*, 3(5):341–351.
- [Rybkin et al., 2021] Rybkin, A., Nicolsky, D., Pelinovsky, E., and Buckel, M. (2021). The generalized Carrier-Greenspan transform for the shallow water system with arbitrary initial and boundary conditions. *Water Waves*, 3:267–296.
- [Rybkin et al., 2024] Rybkin, A., Pelinovsky, E., Bobrovnikov, O., Palmer, N., Pniushkova, E., and Abramowicz, D. (2024). Inverse non-linear problem of the long-wave run-up on coast. *Journal of Ocean Engineering and Marine Energy*, 10(4):941–952.
- [Rybkin et al., 2014] Rybkin, A., Pelinovsky, E., and Didenkulova, I. (2014). Non-linear wave run-up in bays of arbitrary cross-section: generalization of the Carrier-Greenspan approach. *J. Fluid Mech.*, 748:416–432.
- [Rybkin et al., 2023] Rybkin, A., Pelinovsky, E., and Palmer, N. (2023). Inverse problem for the nonlinear long wave runup on a plane sloping beach. *Appl. Math. Lett.*, 145.
- [Satake, 2022] Satake, K. (2022). *Tsunamis, Inverse Problem of*, pages 71–89. Springer US, New York, NY.
- [Shimozono, 2016] Shimozono, T. (2016). Long wave propagation and run-up in converging bays. *J. Fluid Mech.*, 798:457–484.
- [Synolakis and Bernard, 2006] Synolakis, C. and Bernard, E. (2006). Tsunami science before and beyond Boxing Day 2004. *Philos. Trans. Royal Soc.*, 364:2231–2265.
- [Valiani and Caleffi, 2024] Valiani, A. and Caleffi, V. (2024). A one-dimensional augmented shallow water equations system for channels of arbitrary cross-section. *Advances in Water Resources*, 189:104735.
- [Voronin et al., 2015] Voronin, V. V., Voronina, T. A., and Tcheverda, V. A. (2015). Inversion method for initial tsunami waveform reconstruction. *Natural Hazards and Earth System Sciences*, 15(6):1251–1263.
- [Wang et al., 2019] Wang, X., Li, G., Qian, S., Li, J., and Wang, Z. (2019). High order well-balanced finite difference WENO schemes for shallow water flows along channels with irregular geometry. *Applied Mathematics and Computation*, 363:124587.
- [Welahettige et al., 2018] Welahettige, P., Vaagsaether, K., and Lie, B. (2018). A solution method for one-dimensional shallow water equations using flux limiter centered scheme for open Venturi channels. *The Journal of Computational Multiphase Flows*, 10(4):228–238.